

## Hall and Seebeck profiling: Determining surface, interface, and bulk electron transport properties in unintentionally doped InN

Oliver Bierwagen,\* Soojeong Choi, and James S. Speck

*Materials Department, University of California, Santa Barbara, California 93106, USA*

(Received 28 September 2011; published 1 December 2011)

A method for depth profiling of the resistivity, carrier concentration, carrier mobility, and Seebeck coefficient is proposed. This method is based on the measured sheet resistance, Hall coefficient, and Seebeck coefficient of a series of samples with different thicknesses, and data analysis based on multilayer models. We applied this profiling to separate the bulk electron transport properties—concentration, activation energy, mobility, and Seebeck coefficient—of unintentionally doped *n*-type InN from the contribution of the parasitic surface electron accumulation layer and a highly conductive interface region. The  $\approx 200$ -nm-thick interface region shows a high but rapidly decreasing carrier concentration. The dependence of the Seebeck coefficient on electron concentration was extracted. The limits and applicability of this method to extract *p*-type InN transport properties are discussed.

DOI: [10.1103/PhysRevB.84.235302](https://doi.org/10.1103/PhysRevB.84.235302)

PACS number(s): 73.61.Ey, 73.50.Jt, 73.50.Lw, 72.20.-i

### I. INTRODUCTION

Hall measurements are a commonly used tool to determine carrier transport properties, such as carrier type and concentration. These measurements are routinely combined with resistivity measurements. The carrier mobility can then be extracted from resistivity and carrier concentration. Typically used geometries for these combined measurements are the Hall bar geometry and the experimentally more convenient van der Pauw geometry.<sup>1</sup> With the measured Hall data an apparent carrier concentration is calculated, which represents the true carrier concentration as long as the sample contains only one carrier type (either single sheet carrier system or homogenous bulk carrier concentration) with unique, homogenous, and isotropic mobility. While an in-plane anisotropy has no influence on the apparent carrier concentration obtained in Hall bar geometry<sup>2</sup> or van der Pauw geometry,<sup>3</sup> in-plane inhomogeneities could even result in determination of the wrong apparent carrier type using nonstandard contact placement in the van der Pauw geometry.<sup>4</sup> The results of Hall measurements in samples with carrier type or mobility that change with sample thickness (but are assumed to be laterally uniform), i.e., layers with different charge carrier systems, has been worked out by Petritz.<sup>5</sup> In this multilayer case, the apparent carrier concentration generally does not agree with the carrier concentration integrated over the entire sample thickness, but rather shows a strong preference toward the carriers with higher mobility. InN is a material with such characteristics.

InN is the lowest band gap III-nitride material with great potential for electronics applications. The InN bulk transport properties, which are relevant to applications and basic understanding of the material, are not straightforward to measure because the surface electron accumulation layer of InN forms a parallel, parasitic conduction path. The existence of this few-nm-thick accumulation layer with a sheet carrier concentration around  $2 \times 10^{13} \text{ cm}^{-2}$  has been shown by contact studies and electrochemical capacitance-voltage profiling,<sup>6</sup> and by electron-energy-loss spectroscopy.<sup>7</sup> Approaches to separate bulk and parasitic conductivity have been based on the analysis of transport data from thickness series, Shubnikov–de Haas oscillations, or quantitative mobility spectrum analysis

(QMSA) of variable magnetic field conductivity and Hall measurements. In the case of variable thickness series,<sup>6,8</sup> it has been assumed that the measured sheet carrier concentration is the integral of the three-dimensional (3D) carrier concentration over the entire sample thickness (which is only valid if the mobility does not change over the sample thickness), and extrapolation to zero thickness has been used to estimate the surface accumulation transport properties. The QMSA approach has typically yielded two distinct electron species. One species with high mobility has been attributed to bulk carriers,<sup>9–12</sup> whereas the low mobility species has been attributed to the surface carriers<sup>11,12</sup> or the combination of surface and interface carriers.<sup>9,10</sup> The uncertainty about surface or interface carriers could not be resolved by the QMSA method alone. Comparison of the transport results of thin and very thick samples<sup>13</sup> and the more sophisticated fitting of a multilayer, parallel-conduction Petritz model to published thickness dependent transport measurement<sup>14</sup> have strongly suggested the existence of a highly conductive interface region in addition to the surface accumulation layer. Very recently, Shubnikov–de Haas oscillation measurements at high magnetic fields<sup>15</sup> allowed one to identify the sheet surface electron system, bulk electrons, and another electron system that is very likely due to the interface region. All these methods, however, do not yield information on the depths of the electron systems.

In the present study, we determine the depth profile of transport properties by applying the inverted version of the multilayer Petritz model<sup>5</sup> with samples of different thickness. We further extend this method to the profiling of the Seebeck coefficient. As a result, we separate the bulk electron transport properties—concentration, activation energy, mobility, and Seebeck coefficient—of unintentionally doped (uid) *n*-type InN from the contribution of the parasitic electron system, which is confirmed to not only consist of the surface accumulation but also of a roughly 200-nm-thick highly conductive interface region. To corroborate the carrier concentration profile, we use the Seebeck coefficient, which is easy to measure and has an approximately logarithmic dependence<sup>16</sup> on volume carrier concentration.

## II. PROFILING USING MULTILAYER HALL AND SEEBECK MODEL

In Ref. 5, Petritz has theoretically derived the influence of multiple, fully connected layers with charge carriers of different mobility on the apparent transport properties obtained through conductivity and Hall measurements of the entire layer stack. (The case of limited connection between the layers has been treated in Ref. 17.) The inversion of the Petritz model has been applied in Hall profiling, which determines the carrier concentration and mobility of thin sample slices by taking Hall measurements before and after etching away these slices.<sup>18</sup> This method has been implemented in a dedicated Hall profiling system.<sup>19</sup> For InN, it would be difficult to apply this original Hall profiling method due to the difficulty of wet chemical etching,<sup>20</sup> homogeneity issues and alteration of the surface accumulation layer with electrochemical etching,<sup>21</sup> and the likely damage by reactive ion etching. Instead, we use the Hall profiling method with multiple samples grown to different thicknesses, but under otherwise identical growth conditions. We further extend the method to “Seebeck profiling.”

*Layer stack and extraction of one layer.* Figure 1 shows the schematics of two samples with different thickness but otherwise identical properties. The left sample consists of multiple layers that can have different individual transport properties: sheet conductance  $\sigma_i$ , Seebeck coefficient  $S_i$ , and carrier mobility  $\mu_i$ . The right sample comprises an additional layer (accommodating the thickness difference of these two samples) with transport properties of interest  $\sigma_n, S_n, \mu_n$ . In the following, we will show how these transport properties of interest can be extracted from the apparent transport properties of the thick sample ( $\sigma_{\text{tot}}, S_{\text{tot}}, \mu_{\text{tot}}$ ) and those of the thinner sample ( $\sigma_A, S_A, \mu_A$ ). Surprisingly, the thinner sample can be considered as a single layer (despite being composed of multiple different layers) with its apparent transport properties serving as effective single-layer transport properties. Thus the profiling collapses to an effective two-layer problem.

Note that, for simplicity, we consider the sheet conductance and sheet carrier concentration for each layer. This consideration does not limit the validity of the multilayer model and, for bulklike layers, the sheet conductance and sheet carrier concentration  $\sigma_i$  and  $n_i$ , respectively, can be calculated as  $n_i = n_i^{3D} t_i$  and  $\sigma_i = en_i \mu_i$  using the respective 3D carrier concentration  $n_i^{3D}$  and layer thickness  $t_i$ . The sheet conductance is the inverse of the sheet resistance.

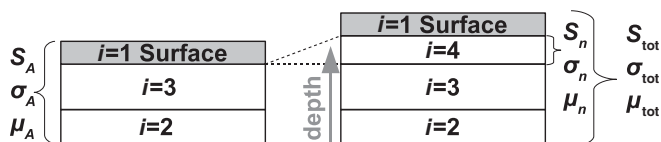


FIG. 1. Schematic layer composition of two films with different thickness. The “Surface” region, marked separately, is present in all films and is likely to have different transport properties than the other layers. In this example, the transport properties of the layer 4 (transport properties denoted by subscript “n”) in the thicker film are extracted by using the apparent transport properties (denoted by subscripts “A” and “tot”) of both films. The depth used in our profiling method refers to the distance to the (insulating) substrate.

*Sheet conductance/resistivity.* The apparent sheet conductance  $\sigma_{\text{tot}}$  measured for multiple layers  $i$  connected in parallel is the sum of their individual sheet conductances  $\sigma_i$ :

$$\sigma_{\text{tot}} = \sum_{i=1}^n \sigma_i = \sigma_A + \sigma_n \quad \text{with} \quad \sigma_A = \sum_{i=1}^{n-1} \sigma_i. \quad (1)$$

Hence the sheet conductance of the layer of interest can be calculated by

$$\sigma_n = \sigma_{\text{tot}} - \sigma_A. \quad (2)$$

With the thickness  $t_n$  of the layer of interest, one can calculate its resulting average resistivity:  $\rho_n = t_n / \sigma_n$ .

*Seebeck coefficient.* When measuring layers (or carrier types)  $i$  with different Seebeck coefficient  $S_i$  in parallel, the apparent Seebeck coefficient  $S_{\text{tot}}$  is the sheet-conductance-weighted average of the individual layer contributions (generalization of the electrons + holes case in Ref. 22):

$$S_{\text{tot}} = \frac{\sum_{i=1}^n \sigma_i S_i}{\sum_{i=1}^n \sigma_i} = \frac{\sum_{i=1}^n \sigma_i S_i}{\sigma_{\text{tot}}} = \frac{\sigma_A S_A + \sigma_n S_n}{\sigma_A + \sigma_n}. \quad (3)$$

With  $S_A = \sum_{i=1}^{n-1} \sigma_i S_i / \sum_{i=1}^{n-1} \sigma_i$ , we can extract the Seebeck coefficient for the layer of interest as

$$S_n = \frac{\sigma_{\text{tot}} S_{\text{tot}} - \sigma_A S_A}{\sigma_n}. \quad (4)$$

*Mobility (Hall).* According to Refs. 5 and 17, the apparent mobility  $\mu_{\text{tot}}$  of a stack of fully connected layers is

$$\mu_{\text{tot}} = \frac{\sum_{i=1}^n \sigma_i \mu_i}{\sum_{i=1}^n \sigma_i} = \frac{\sum_{i=1}^n \sigma_i \mu_i}{\sigma_{\text{tot}}}. \quad (5)$$

Using  $\mu_A = \sum_{i=1}^{n-1} \sigma_i \mu_i / \sum_{i=1}^{n-1} \sigma_i = \sum_{i=1}^{n-1} \sigma_i \mu_i / \sigma_A$ , we can rewrite  $\mu_{\text{tot}} = (\sigma_A \mu_A + \sigma_n \mu_n) / (\sigma_A + \sigma_n)$  and extract the mobility of the layer of interest as

$$\mu_n = \frac{\sigma_{\text{tot}} \mu_{\text{tot}} - \sigma_A \mu_A}{\sigma_n}. \quad (6)$$

The apparent carrier concentration  $n_{\text{tot}}$  of the stack can be obtained by rewriting Eq. (5) into its equivalent:

$$n_{\text{tot}} = \frac{\sum_i \mu_i^2 n_i}{\mu_{\text{tot}}^2} = \frac{(\sum_i \mu_i n_i)^2}{\sum_i \mu_i^2 n_i}. \quad (7)$$

In this equation, the  $\mu^2$  weighing factor leads to a deviation of the apparent carrier concentration  $n_{\text{tot}}$  from the integrated carrier concentration  $\sum_i n_i$  toward the (lower) concentration of the carriers with higher mobility.

## III. EXPERIMENT

A series of uid InN films with thicknesses ranging from 10 to 800 nm (10, 20, 50, 100, 200, 400, 800 nm) was grown by plasma-assisted molecular beam epitaxy (PA-MBE). The films were grown on a 100-nm-thick C-doped (semi-insulating) GaN buffer layer on a semi-insulating  $c$ -plane GaN:Fe template (Lumilog). The InN growth rate was 300 nm/h at a substrate temperature of 440–450 °C (measured by pyrometer) under In-rich growth conditions. Square-shaped chips were cleaved from the grown samples and contacted by pressing In dots on the InN surface in the corners.

Room-temperature (RT) thermoelectric measurements were performed by applying a variable temperature difference to two opposite edges of the chips using Peltier elements, and measuring the thermovoltage between two contacts—one on each of these edges. The temperature at these contacts was measured by thermocouples brought into contact with the sample surface next to the contacts used for thermovoltage measurement. The thermovoltage  $V_{th}$  follows a linear relation with the temperature difference  $\Delta T$ , and the Seebeck coefficient of the sample-wire combination  $S - S_{wire} = dV_{th}/d\Delta T$  was determined as the slope to exclude any offset voltages. The contribution  $S_{wire}$  due to the indium contacts and copper wires (Seebeck coefficients on the order of  $2 \mu\text{V/K}$ ) is smaller than  $10 \mu\text{V/K}$ . Since this value is much smaller than the Seebeck coefficient of the sample  $S$  (on the order of  $100 \mu\text{V/K}$ ), we neglected  $S_{wire}$ .

Conductivity and Hall measurements in van der Pauw geometry<sup>1</sup> were performed with the samples at temperatures between 300 K (RT) and 25 K using a dc current of  $100 \mu\text{A}$ , magnetic field of 0.5 T, and standard current and magnetic field reversal to exclude any parasitic offset voltages. The measured sheet resistance  $R_S$  ( $\Omega/\square$ ) was converted into the sample sheet conductance  $\sigma = 1/R_S$ . Hall measurements proceeded by passing an in-plane current  $I$  through the sample and measuring the in-plane Hall voltage  $V_H$  (perpendicular to the current direction) caused by an out-of-plane magnetic field (perpendicular to the sample). The measured Hall coefficient  $R_H = V_H/(IB)$  was then used to calculate the apparent carrier concentration  $n = r_H/(eR_H)$ , and the apparent mobility  $\mu = R_H/(r_H R_S)$  with Hall scattering factor  $r_H$ . The Hall scattering factor depends of the detailed scattering mechanisms at play and can theoretically assume values between 1 and 2. In most cases,  $r_H \approx 1$ , and particularly for degenerate carrier systems  $r_H = 1$ . Our results suggest the degenerate carrier case for InN and we are hence assuming  $r_H$  unity.

#### IV. RESULTS AND DISCUSSION

Figure 2 shows the RT apparent sheet conductance and sheet electron concentration measured for the samples of different thickness.

*Surface accumulation and nonlinear thickness dependence.* For the thinnest (10-nm-thick) sample, the transport properties should be mainly influenced by the surface accumulation. Hence the sheet resistance of  $1.2 \text{ k}\Omega$ , sheet carrier concentration of  $2.8 \times 10^{13} \text{ cm}^{-2}$ , and corresponding mobility of  $200 \text{ cm}^2/\text{Vs}$  can be regarded an estimate of the accumulation layer transport properties. Within a factor of 2, these values agree with all those extracted by several methods.<sup>9,14,15,21</sup> The low magnitude of Seebeck coefficient ( $-37 \mu\text{V/K}$ ) suggests a high volume carrier concentration. Based on calculations,<sup>16</sup> the Seebeck coefficient corresponds to  $2 \times 10^{19} \text{ cm}^{-3}$ , which is a factor of 4 times smaller than the peak volume concentration calculated for an InN surface accumulation.<sup>14</sup>

With increasing film thickness, the sheet conductance increases—but not linearly—as more InN contributes. The apparent sheet electron concentration, however, shows an initially decreasing value at low thickness before it rises again as expected for increasing thickness. These nonlinearities clearly show that transport properties of the surface accumulation

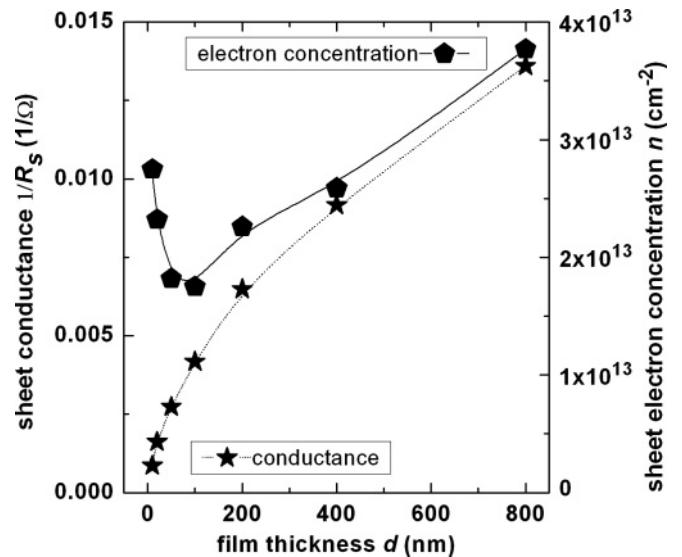


FIG. 2. Apparent sheet conductance and sheet electron concentration as a function of InN film thickness. Lines serve as a guide to the eye.

layer cannot be simply deduced by an extrapolation to zero thickness. The initially decreasing apparent sheet electron concentration can be rather explained by the addition of higher mobility electrons with lower sheet concentration to the low mobility surface electrons for thicker samples: for example, from the profile (discussed next) in Fig. 3, the 40-nm-thick layer between a depth of 10 and 50 nm (second to left open circle) has a sheet electron concentration of  $40 \text{ nm} \times 2.3 \times 10^{18} \text{ cm}^{-3} = 0.92 \times 10^{13} \text{ cm}^{-2}$  at a mobility of  $1280 \text{ cm}^2/\text{Vs}$ . With this layer parallel to the surface (apparent transport properties of the 10 nm sample), Eq. (7) yields a total apparent sheet electron concentration of  $\approx 1.9 \times 10^{13} \text{ cm}^{-2}$ , which is in fact smaller than that of the surface only. Once the sheet concentration of the high-mobility electrons is high enough (layer is thick enough), its increase also results in an increasing apparent electron concentration.

*Depth profile.* Figure 3 shows the results of the depth profiling based on the multilayer model (“multilayer”) as introduced in Sec. II. For comparison, we included the apparent data points (“apparent”, treating the sample as a homogeneous single layer). It is obvious that the assumption of a homogeneous layer would lead to an underestimation of the resistivity, the mobility, and the magnitude of Seebeck coefficient with simultaneous overestimation of the volume carrier concentration. The depth of the profile data points is the average of the thicknesses of the two films used for the calculation of the data point. For example, the extracted transport properties using the 50-nm- and the 100-nm-thick sample describe a 50-nm-thick slab with center at a depth of 75 nm. Note that the depth refers to the distance to the substrate interface. In the profile data, two different regions can be discerned: a region with rapidly changing properties at depths below  $\approx 200 \text{ nm}$ , and a region with quite constant transport properties at larger depths.

*Interface region.* A minimum resistivity and maximum carrier concentration (several  $10^{18} \text{ cm}^{-3}$ ) with low magnitude of Seebeck coefficient and low mobility is found at the lowest depths (close to the substrate). With increasing depth,

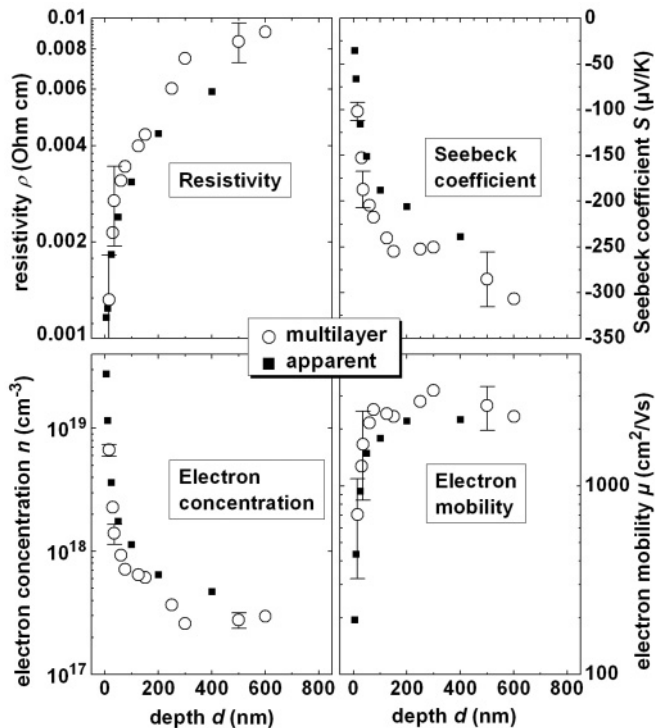


FIG. 3. RT electron transport properties: resistivity (top left), Seebeck coefficient (top right), volume concentration (bottom left), and mobility (bottom right) extracted from the measurements based on the profiling method (open symbols). The profiling data is plotted as a function of distance between the center of the layer of interest and the substrate ( $d$ ). For comparison, the apparent data (assuming a single homogeneous layer) is plotted (solid symbols).

the resistivity rapidly increases and the carrier concentration decreases accordingly with simultaneous increase in mobility and magnitude of Seebeck coefficient. This drastic change in transport properties takes place on a length scale of  $\approx 100$  nm, which is much larger than the surface accumulation layer thickness ( $\approx 3$  nm<sup>14</sup>). Therefore, these rapidly changing transport properties cannot be explained by profiling the accumulation layer, and this profile is rather caused by the (dislocated) interface region of the InN layer on GaN. The fact that the Seebeck coefficient at a depth of 15 nm (Fig. 3 top right, top open disk) is already three times larger than that of the surface (Fig. 3 top right, top solid square) signifies a substantially lower volume carrier concentration in the interface region than in the surface accumulation layer. The mobilities that we obtained for the surface and the interface region suggest that the broad low mobility peak (ranging from  $\approx 300$  to  $\approx 1000$  cm<sup>2</sup>/Vs) in the QMSA spectra of Refs. 11 and 12 correspond to a superposition of surface (low mobility side of peak) and interface carrier peaks (high mobility side of peak) rather than just the surface carrier peak.

For InN, the increased conductivity at interface regions of InN on GaN has already been suggested in Ref. 13 by comparing single-layer Hall data of a 128-nm- and a 12- $\mu$ m-thick sample, by the multilayer modeling of Ref. 14, and has been attributed to dislocations acting as donors in InN. A highly conductive interface region also exists in other materials, e.g., in uid SnO<sub>2</sub>,<sup>23</sup> and coincides with a high density

of dislocations in this region.<sup>24</sup> The thickness of the highly conductive interface region is an important quantity for future sample or device design.

*Bulk region.* At depths above  $\approx 300$  nm, the transport properties are quite depth-invariant and are thus considered those of the bulk (i.e., not influenced by the interface or surface anymore). The extracted bulk volume carrier concentration is  $(2.8 \pm 0.2) \times 10^{17}$  cm<sup>-3</sup> at mobilities of  $(2700 \pm 500)$  cm<sup>2</sup>/Vs and a high magnitude Seebeck coefficient of  $-(280 \pm 30)$   $\mu$ V/K. The bulk carrier concentration and mobilities are comparable to those obtained by the QMSA method on similar samples.<sup>12</sup>

An additional InN sample was grown consisting of 1  $\mu$ m uid InN on top of a 1- $\mu$ m-thick InN acceptor doped with  $9 \times 10^{17}$  cm<sup>-3</sup> Mg. The Mg doping serves to make the interface region semi-insulating by compensation.<sup>25</sup> Hence the apparent transport properties are less influenced by low-mobility electrons and are more representative of the bulk properties. Transport measurements of this sample yielded an apparent mobility of 2870 cm<sup>2</sup>/Vs, which is in good agreement with our profile data from the bulk region of the uid thickness series.

*Temperature dependence.* The temperature dependence of the transport properties (volume carrier concentration and mobility) is given in Fig. 4. The electron concentration of the 10-nm sample is temperature invariant, but the mobility shows a slight initial increase from 300 to 150 K but an otherwise constant mobility. These data suggest a degenerate surface accumulation layer whose mobility (around 200 cm<sup>2</sup>/Vs) has some minor phonon scattering contribution.

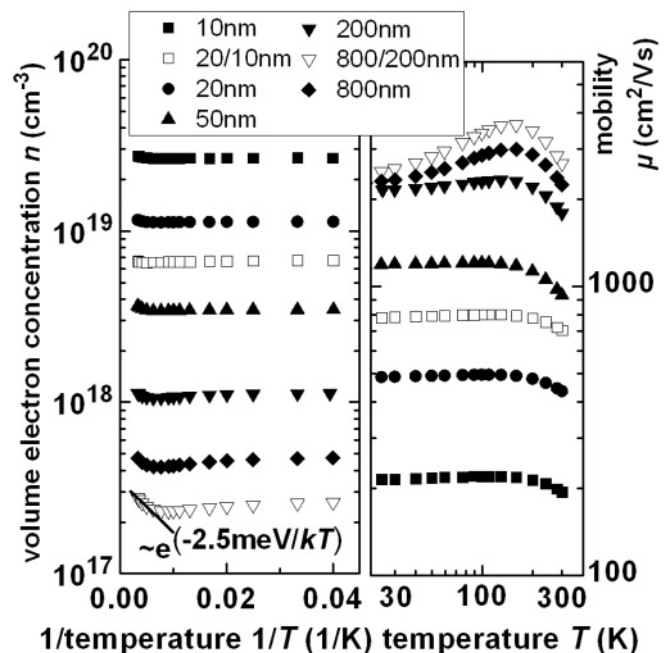


FIG. 4. Volume electron concentration (left) and electron mobility (right) as a function of temperature. The apparent transport properties using the single-layer interpretation (solid symbols), and two different sample regions (close to the interface at 10–20 nm and in the bulk at 200–800 nm) extracted by the profiling method (open symbols) are shown.

The profiling data extracted from the 10 and 20 nm sample, corresponding to the interface region 15 nm away from the interface, shows a degenerate electron concentration of  $7 \times 10^{18} \text{ cm}^{-3}$ , but at a significantly higher mobility than the surface. The temperature dependence of the mobility is qualitatively the same as that of the surface, but at a higher magnitude (it increases from 700 to  $800 \text{ cm}^2/\text{V s}$  between 300 and 150 K). This distinctly higher mobility confirms that the electron system at 15 nm is different from that of the surface.

A qualitatively different behavior is observed in the bulk region at a distance of 500 nm from the interface (extracted from the 200 and 800 nm samples). Here a slight freeze-out with activation energy of 2.5 meV is observed between 300 and 150 K followed by a slight freeze-in, which might indicate a transition to donor-band conductivity as also observed in  $\text{In}_2\text{O}_3$ .<sup>26</sup> Whether this freeze-out is real or is an artifact of a changing Hall scattering factor  $r_H$  (that increases as the phonon scattering contribution decreases and that of ionized impurity scattering increases) is still questionable. We may, however, conclude that the donor binding energy in InN is on the order of 1 meV<sup>10</sup> or the volume carrier concentration of almost  $3 \times 10^{17} \text{ cm}^{-3}$  is still degenerate.<sup>14</sup> The mobility in the bulk region increases from 2700 to  $3600 \text{ cm}^2/\text{V s}$  between 300 and 150 K, being limited by phonon scattering before it decreases again to  $2500 \text{ cm}^2/\text{V s}$  at 25 K as ionized impurity scattering or charged dislocation scattering are dominant. This mobility is significantly higher at a simultaneously lower electron concentration than that of the interface region, which would be in agreement with near interface dislocations acting as donors and scatterers.

**Role of dislocations.** The role of dislocations as uid donors and scattering centers in InN is still unresolved. Experimental studies comparing measured dislocation densities to electron concentrations<sup>27,28</sup> concluded that unintentional impurities rather than dislocations are the source of electrons, but dislocations act as scatterers to limit the electron mobility. Very recently, first principle calculations<sup>29</sup> have designated electronic states of threading dislocations as a source of electrons, and the impact of dislocation scattering on Seebeck coefficient and electron mobility has been calculated<sup>16</sup> and compared to experimental data. While Ref. 29 does not give the relation of dislocation density to electron density, Ref. 16 assumes dislocation lines to act as one donor or one acceptor per  $c$ -lattice parameter ( $5.7 \text{ \AA}$ ), corresponding to a volume donor or acceptor concentration of  $1.75 \times 10^{17} \text{ cm}^{-3}$  for a dislocation density of  $10^{10} \text{ cm}^{-2}$ . In transport calculations, Ref. 16 accommodates a discrepancy between dislocation-caused donors or acceptors and electron concentration by a suitable concentration of additional donors or acceptors. Dislocation densities measured by transmission electron microscopy (TEM) in InN typically range from  $10^9$  to  $10^{11} \text{ cm}^{-2}$  (Ref. 16), and the fraction of electrons from assumed dislocation donors in that study ranged from 0.15 to 0.49.

The threading dislocation density in our samples is likely on the order of  $(1-2) \times 10^{10} \text{ cm}^{-2}$ , and the corresponding theoretical donor concentration of  $(1.75-3.5) \times 10^{17} \text{ cm}^{-3}$  would be in good agreement with the bulk electron concentration determined by the profiling method (cf. Fig. 3). The approximately one order of magnitude higher electron

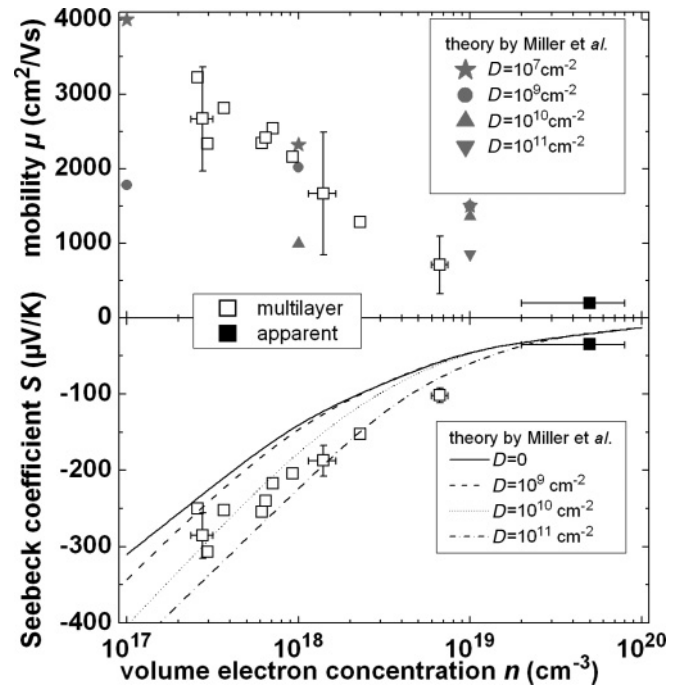


FIG. 5. InN electron mobility and Seebeck coefficient at RT as a function of volume electron concentration. Since the data was compiled from profiles given in Fig. 3, the data points correspond to different depths in the sample. The data point at the highest concentration corresponds to the measured data of the thinnest sample with the error bar of the carrier concentration ranging from the single layer assumption of a pure accumulation layer (high concentration side, more likely) to that of a homogeneous distribution of the charge and no accumulation layer (low concentration side). The lowest concentration data points are several 100 nm away from the interface and considered the bulk properties. For comparison, the results of theoretical calculations of Ref. 16 are given.

concentration in the interface region is compatible with the rapid drop of dislocation density in the first few 100 nm from the substrate interface.<sup>16</sup>

Figure 5 summarizes the dependence of the electron mobility  $\mu$  and the Seebeck coefficient  $S$  on volume carrier concentration  $n$  using our profile data of different depths, and compares them to the theoretical calculations of Ref. 16. The approximately logarithmic dependence of  $S$  on  $n$  is obvious by the semilog plot, and the comparison to the theoretical curves of Ref. 16 is very favorable. We can even observe the trend of our data from corresponding to a high dislocation density ( $10^{11} \text{ cm}^{-2}$ ) in the interface region (high electron concentrations) to corresponding to a lower dislocation ( $10^{10} \text{ cm}^{-2}$ ) for the bulk region (low electron concentrations).

The mobility dependence on electron (and hence donor) concentration given in Fig. 5 shows an increasing mobility with decreasing electron concentration (and simultaneous increasing distance to the substrate interface). This dependence would be typical for ionized impurity scattering in which an increasing concentration of ionized donors increased electron concentration but simultaneously decreased the mobility by scattering. The agreement with the theoretically calculated mobility of Ref. 16 as function of electron concentration and

dislocation density is approximate for the electron concentrations between  $10^{18}$  and  $10^{19}$   $\text{cm}^{-3}$  (interface region) but at lower electron concentrations (in the bulk region) and, for typically measured InN dislocation densities, the theory predicts a significantly lower mobility than experimentally observed. Solely, unrealistically low dislocation densities around  $10^8$   $\text{cm}^{-2}$  or a decreased donor density with one donor every  $100 \times c$ -lattice constant along dislocation lines would be able to model our determined mobilities in the bulk region.

Summarizing, our electron concentration data is compatible with dislocations forming one uid donor every  $c$ -lattice constant along the dislocation line in our InN samples, which is corroborated by the Seebeck data in light of the theory from Ref. 16. On the other hand, the theoretical predictions of the same reference on mobility as a function of dislocation density and electron concentrations are significantly lower than our experimental results. This discrepancy suggests that either the used model does not represent the real samples or the donor density along dislocation lines is orders of magnitude lower than expected and there is an additional source of electrons such as impurities (suggested by Refs. 27 and 28). Hence, with the present data, it is not possible to unambiguously assign the uid donors in InN to either dislocation or impurities.

*Uncertainties.* The basic assumption for the profiling method with a variable thickness series of samples is that the growth is reproducible in terms of electrical properties of the layers (see also Fig. 1). Due to the presence of the surface accumulation layer, an additional assumption is that this accumulation layer is independent of the underlying film thickness.

To get a quantitative impression of the achievable uncertainties, we plotted error bars for selected profile data points in Figs. 4 and 5. These error bars were calculated for relative uncertainties of the measured sheet resistance and carrier concentration values of 5%—i.e., also the reproducibility had to be within these 5%. Based on Eqs. (2), (4), and (6), it is obvious that the reliability of the results rises with increasing difference in transport properties between the two samples used to calculate the profile data point.

## V. APPLICABILITY TO $p$ -DOPED InN

Measuring transport properties of  $p$ -type InN is still challenged by the presence of the  $n$ -type surface accumulation layer. While a positive apparent Seebeck coefficient has already been measured in  $p$ -doped layers,<sup>30,31</sup> Hall measurements result in an apparent total concentration of electrons instead of holes. The reason for the discrepancy between Seebeck and Hall measurements is based on the mobility factor that weighs the respective (bulk)hole and (surface)electron contributions of opposite sign. This weighing factor is linear in the case of Seebeck [linear contribution to  $\sigma$  in the numerator of Eq. (3)] and quadratic for Hall measurements [sign-determining denominator of Eq. (7)]. Due to the relatively lower hole mobility (probably on the order of  $10$   $\text{cm}^2/\text{V s}$ ) than that of the surface electrons (on the order of  $100$   $\text{cm}^2/\text{V s}$ ), an  $\approx 100$  times higher (hence  $> 3 \times 10^{15}$   $\text{cm}^{-2}$ ) sheet bulk hole concentration than surface electron concentration would be necessary to observe apparent holes in single-layer Hall

measurements. (Note that for a volume hole concentration of  $10^{18}$   $\text{cm}^{-3}$ , this would correspond to a  $20$ - $\mu\text{m}$ -thick  $p$ -doped InN layer.) In addition, the highly unintentionally  $n$ -type doped interface region might provide an additional parasitic  $n$ -type channel if the acceptor concentration is too low to compensate all donors in this region (see also Ref. 25).

While the difference between our profiling data and the apparent data obtained without the profiling method is typically smaller than a factor of 2 (see Fig. 3), the profiling method can make a decisive difference for  $p$ -doped InN. In fact, the profiling method is able to extract the  $p$ -type transport properties from samples of different thicknesses that individually show apparent  $n$ -type properties by Hall measurements. In all our equations, positive carrier concentrations  $n$  and mobilities  $\mu$  correspond to electrons, whereas negative values correspond to holes. Since all our equations also hold true for a mix of  $p$ -type and  $n$ -type carrier systems, the Hall profiling method presented here bears the chance to extract InN bulk hole transport properties under the assumption that the surface electron and bulk hole systems are electrically connected (likely given as this requirement also holds for the successful  $p$ -type Seebeck measurements). In order to obtain reliable results, however, the  $\sigma_n \mu_n$  product of the  $p$ -type slab in Eq. (6) (see also Fig. 1) has to be in excess of the uncertainty of the  $\sigma_{\text{tot}} \mu_{\text{tot}}$  and  $\sigma_A \mu_A$  product of the full samples. This condition is far more relaxed than that to observe  $p$ -type conductivity in the single-layer model by scaling the necessary  $p$ -layer thickness for the single layer model by the relative uncertainty of the  $\sigma \mu$  products mentioned above. Experimentally, this calls for thick (e.g., order of  $1$   $\mu\text{m}$ ), highly  $p$ -doped layers.

## VI. SUMMARY

In summary, we presented a method to determine the depth profile of transport properties (resistivity, carrier concentration, mobility, and Seebeck coefficient) that is based on a simple multilayer analysis and samples of different thickness.

This profiling method was applied to unintentionally doped  $n$ -type InN thin films grown on semi-insulating GaN, and allowed us to identify three different electron systems.

- (1) The degenerate surface accumulation layer with a sheet electron concentration of  $2.8 \times 10^{13}$   $\text{cm}^{-2}$ , electron mobility of  $200$   $\text{cm}^2/\text{V s}$ , and Seebeck coefficient of  $-37$   $\mu\text{V}/\text{K}$ .
- (2) The bulk region with a RT volume carrier concentration of  $2.8 \times 10^{17}$   $\text{cm}^{-3}$ , mobility of  $2700$   $\text{cm}^2/\text{V s}$ , and Seebeck coefficient of  $-280$   $\mu\text{V}/\text{K}$ . These bulk electron mobilities are higher and bulk electron concentrations are lower than the respective apparent values. The freeze-out of the bulk electrons with an activation energy as low as  $2.5$  meV suggests either extremely shallow donors or degeneracy.
- (3) The (partly) degenerate,  $\approx 200$ -nm-thick highly conductive interface region, with a volume carrier concentration in the high  $10^{18}$   $\text{cm}^{-3}$  range that rapidly decays with distance to the interface.

The presence of the interface region needs to be recognized as its transport properties might be falsely attributed to the surface accumulation layer, and could also contribute to parasitic  $n$ -type conductivity in acceptor-doped samples.

The Seebeck coefficient for the volume carrier concentrations found in the sample ( $\approx 3 \times 10^{17} \text{ cm}^{-3}$  to  $\approx 1 \times 10^{20} \text{ cm}^{-3}$ ) was extracted by the profiling method and is in good agreement with theoretically modeled values of Ref. 16. In contrast, the electron mobilities (apparent and extracted by profiling) of the bulk region are significantly higher than the theoretically modeled ones of Ref. 16.

Uncertainties of the profiling method were discussed. Guidelines on how to use this method to determine *p*-type InN

transport properties despite an apparent *n*-type conductivity (due to the strong surface electron accumulation layer) were given.

#### ACKNOWLEDGMENTS

We thank Ashok T. Ramu for help with the Seebeck measurement. O.B. was supported by AFOSR Grant No. FA9550-08-1-0461.

\*Also at Paul-Drude-Institut für Festkörperelektronik, Hausvogteiplatz 5-7, D-10117 Berlin, Germany.

<sup>1</sup>L. J. van der Pauw, Philips Research Reports **13**, 1 (1958).

<sup>2</sup>H. Shibata and J. Oide, *J. Appl. Phys.* **88**, 4813 (2000).

<sup>3</sup>O. Bierwagen, R. Pomraenke, S. Eilers, and W. T. Masselink, *Phys. Rev. B* **70**, 165307 (2004).

<sup>4</sup>O. Bierwagen, T. Ive, C. G. Van de Walle, and J. S. Speck, *Appl. Phys. Lett.* **93**, 242108 (2008).

<sup>5</sup>R. L. Petritz, *Phys. Rev.* **110**, 1254 (1958).

<sup>6</sup>H. Lu, W. J. Schaff, L. F. Eastman, and C. E. Stutz, *Appl. Phys. Lett.* **82**, 1736 (2003).

<sup>7</sup>I. Mahboob, T. D. Veal, C. F. McConville, H. Lu, and W. J. Schaff, *Phys. Rev. Lett.* **92**, 036804 (2004).

<sup>8</sup>W. Liu, R. J. N. Tan, C. B. Soh, and S. J. Chua, *Appl. Phys. Lett.* **97**, 042110 (2010).

<sup>9</sup>C. H. Swartz, R. P. Tompkins, N. C. Giles, T. H. Myers, H. Lu, W. J. Schaff, and L. F. Eastman, *J. Cryst. Growth* **269**, 29 (2004).

<sup>10</sup>C. H. Swartz, R. P. Tompkins, T. H. Myers, H. Lu, and W. J. Schaff, *Phys. Status Solidi C* **2**, 2250 (2005).

<sup>11</sup>T. B. Fehlberg, G. A. Umana-Membreno, B. D. Nener, G. Parish, C. S. Gallinat, G. Koblmüller, S. Rajan, S. Bernardis, and J. S. Speck, *Jpn. J. Appl. Phys., Part 2* **45**, L1090 (2006).

<sup>12</sup>T. B. Fehlberg, C. S. Gallinat, G. A. Umana-Membreno, G. Koblmüller, B. D. Nener, J. S. Speck, and G. Parish, *J. Electron. Mater.* **37**, 593 (2008).

<sup>13</sup>N. Miller *et al.*, *Physica B* **404**, 4862 (2009).

<sup>14</sup>P. D. C. King, T. D. Veal, and C. F. McConville, *J. Phys. Condens. Matter* **21**, 174201 (2009).

<sup>15</sup>T. A. Komissarova, V. N. Jmerik, S. V. Ivanov, O. Drachenko, X. Wang, and A. Yoshikawa, *Phys. Rev. B* **84**, 035205 (2011).

<sup>16</sup>N. Miller, E. E. Haller, G. Koblmüller, C. Gallinat, J. S. Speck, W. J. Schaff, M. E. Hawkrige, K. M. Yu, and J. W. Ager, *Phys. Rev. B* **84**, 075315 (2011).

<sup>17</sup>B. Arnaudov, T. Paskova, S. Evtimova, E. Valcheva, M. Heuken, and B. Monemar, *Phys. Rev. B* **67**, 045314 (2003).

<sup>18</sup>R. Baron, G. A. Shifrin, O. J. Marsh, and J. W. Mayer, *J. Appl. Phys.* **40**, 3702 (1969).

<sup>19</sup>S. R. Blight, R. E. Nicholls, S. P. S. Sangha, P. B. Kirby, L. Teale, S. P. Hiscock, and C. P. Stewart, *J. Phys. E* **21**, 470 (1988).

<sup>20</sup>C. B. Vartuli, S. J. Pearton, C. R. Abernathy, J. D. MacKenzie, F. Ren, J. C. Zolper, and R. J. Shul, *Solid-State Electron.* **41**, 1947 (1997).

<sup>21</sup>A. Denisenko, C. Pietzka, A. Chuvilin, U. Kaiser, H. Lu, W. J. Schaff, and E. Kohn, *J. Appl. Phys.* **105**, 033702 (2009).

<sup>22</sup>K. Seeger, *Semiconductor Physics*, 9th ed. (Springer, New York, 2004).

<sup>23</sup>M. E. White, O. Bierwagen, M. Y. Tsai, and J. S. Speck, *J. Appl. Phys.* **106**, 093704 (2009).

<sup>24</sup>M. E. White, M. Y. Tsai, F. Wu, and J. S. Speck, *J. Vac. Sci. Technol. A* **26**, 1300 (2008).

<sup>25</sup>M. E. White, O. Bierwagen, M.-Y. Tsai, and J. S. Speck, *Appl. Phys. Express* **3**, 051101 (2010).

<sup>26</sup>O. Bierwagen and J. S. Speck, *Appl. Phys. Lett.* **97**, 072103 (2010).

<sup>27</sup>V. Darakchieva *et al.*, *Physica B* **404**, 4476 (2009).

<sup>28</sup>C. S. Gallinat, G. Koblmüller, and J. S. Speck, *Appl. Phys. Lett.* **95**, 022103 (2009).

<sup>29</sup>E. Kalesaki, J. Kioseoglou, L. Lymperakis, P. Komninou, and T. Karakostas, *Appl. Phys. Lett.* **98**, 072103 (2011).

<sup>30</sup>R. E. Jones, K. M. Yu, S. X. Li, W. Walukiewicz, J. W. Ager, E. E. Haller, H. Lu, and W. J. Schaff, *Phys. Rev. Lett.* **96**, 125505 (2006).

<sup>31</sup>N. Miller *et al.*, *J. Appl. Phys.* **107**, 113712 (2010).